JOURNAL OF AEROSPACE COMPUTING, INFORMATION, AND COMMUNICATION
Vol. 1, November 2004

Transmission Capacity Degradation due to Traffic Changes in Interactive Multimedia Satellite Communications

Masayoshi Tanaka*
Nihon University, Narashino, Japan

This paper presents a study on transmission capacity degradation due to traffic distribution changes in an interactive multimedia multibeam satellite communications system (IMMSC). An analytical model for the return link in which the bandwidth is shared with multiple beams and beam couplings exist is discussed and using this model, the effects of adjacent beams and the relationship between traffic distribution and change in transmission linearity are investigated. It is found that the effects of undesired signals leaked from adjacent beams, which up to now have been considered small, cannot be neglected for the return link. They depend on the traffic distribution and cause linearity degradation and a decrease in maximum transmission capacity. Based on the study, effective methods are also presented for increasing the return link access capacity.

I. Introduction

The rapid advance of information technology is reason for the growing demand for high-speed access to the Internet, anytime, anywhere, at a reasonable cost to the consumer. An interactive multimedia multibeam satellite communications system (IMMSC) is one of the promising network access systems because it can be used to construct a broadband access system more easily, more rapidly and in a much wider area, compared with other systems, such as fiber-to-the-home (FTTH), CATV, or ADSL.

During the past several years, more than a dozen satellite systems with dedicated bentpipe/processing payloads, LEO, MEO, GEO constellation, and fixed, moving, or hopping beams have been proposed. The DVB Return Channel System via Satellite (DVB-RCS)[1] is one of them and employs a user terminal supporting a two-way multimedia system.

In IMMSC, user uplink traffic is generally lower than that of user down link; i.e., the traffic is asymmetrical. The bandwidth of the return link (user terminal to hub station) can thus be shared in a group of seven or eight beams and can be dynamically assigned to match the return traffic demand.[2] User terminals can employ a multi-carrier system like Multi-Frequency TDMA (MF-TDMA)[1] as their uplink scheme, which enables bandwidth-on-demand and is a very efficient adaptation to widely varying multimedia transmission requirements.

A multi-carrier system however must possess linearity since its carriers undergo common amplification. Linearity is generally critical in satellite-on-board devices, especially in a high power amplifier (HPA), which is required to operate as near the saturation region as possible to raise efficiency within the range that satisfies system requirements. Hence, degradation in linearity lowers the quality of communications or decreases the maximum number of access channels.

In addition, actual antenna isolation among beams is limited, and as a result, beam couplings exist and leaks from adjacent beams do occur. At the same time, traffic is not uniform across all beams, because users are distributed geographically. Traffic itself, moreover, is characterized by variation over time. Therefore, leaks from adjacent beams change depending on the traffic distribution. However, there have been no reports to fully investigate how beam couplings affect transmission characteristics or proposals for countermeasures to it.

Presented as Paper 2002-1854 at the 20th AIAA International Communications Satellite Systems Conference and Exhibit, Montreal, Canada, 12-15 May 2002; received 13 February 2004; revision received 22 July 2004, accepted for publication 23 August 2004.

*Professor, College of Industrial Technology, Department of Electrical and Electronic Engineering. mtanaka@cit.nihon-u.ac.jp.

Hence, in this paper, the main focus is placed on the return-link transmission system of IMMSC in which couplings among multibeams become a problem. The total amount of undesired signal leakage from adjacent beams is analyzed when the traffic distribution varies. On the basis of this analysis, a theoretical study on the change in characteristics is performed and the items that must be considered in a system design are investigated.

II. □ Concept of IMMSC

The configuration of the IMMSC system is shown in Fig. 1. The payload has the bentpipe architecture and provides independent, star-based, sub-networks, wherein an end-user can communicate to a hub station. For both the user link (the link between the user terminals and the satellite) and the feeder link (the link between the hub stations and the satellite), the uplink beam configuration is identical to the downlink beam configuration. The user link beam configuration consists of many spot beams covering the service area. Every set of several user-link beams is associated with a hub station to form a sub-network.

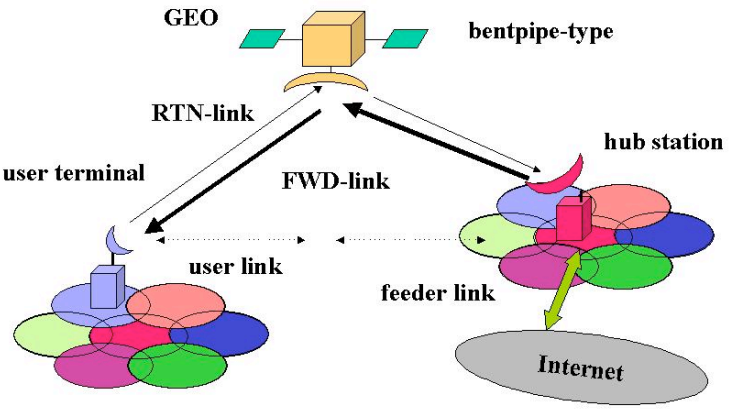

Fig. 1 Configuration of interactive multimedia multi-beam satellite communications system.

The forward link has the traditional transparent bent-pipe architecture. For a group of beams, a hub station uplinks TDM carriers destined for its user-link beams. The user terminal receives signals generated by the satellite hub station. In addition, the interactive system has the capability of transmitting from the user site via the same antenna as for receiving.

The user uplink traffic of IMMSC is generally lower than that of the user downlink; i.e., the traffic is asymmetrical. From the viewpoint of the efficient use of frequency band, a wider bandwidth should be assigned for the forward link to achieve broadband transmission as shown in Fig. 2. For the return link, the bandwidth associated with an uplink beam can be re-configured. Within a group of beams, the uplink bandwidth of a beam can be increased at the expense of uplink bandwidth of another beam. For example, a Multi-Frequency Time Division Multiple Access (MF-TDMA) scheme can be employed for the user terminals to share the capacity available for transmission.

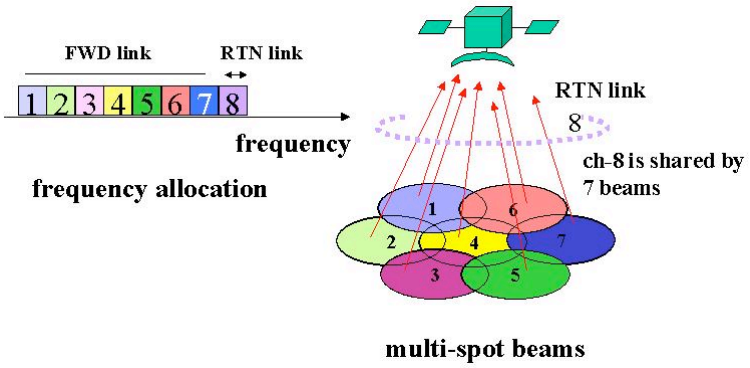

Fig. 2 Frequency allocation for forward link and return link.

In the return link satellite payload (Fig. 3), the signals from each beam are received by receiver units (RX) and are combined at the combiner (COM). These signals are then placed on the feeder-link frequency, and after being

co-amplified by a common transmitter (TX) and a high power amplifier (HPA), are sent out together to the hub station. As a result, signals from each service area overlap in their uplink band and are all co-amplified by the final HPA. In order to alleviate the impact of intermodulation interference on the return link, the HPA should be operated in a linear mode

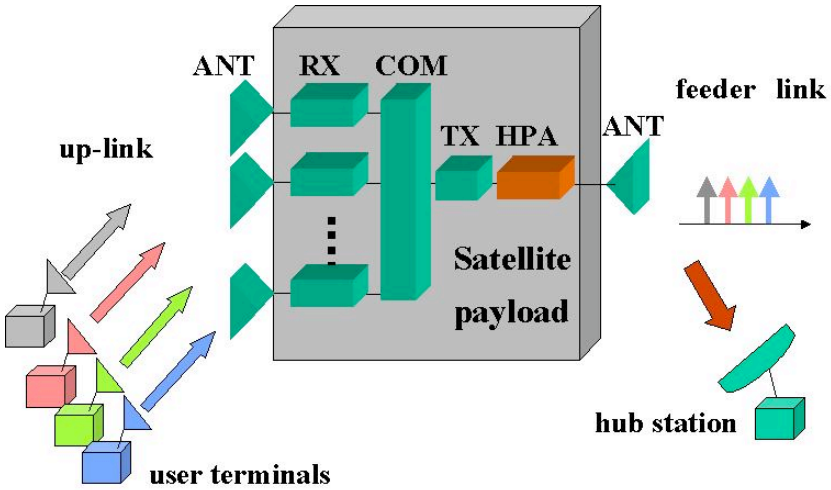

Fig. 3 Configuration of return link payload.

III. Analysis of Return Link

The onboard receiving antennas on a multibeam payload possess a gain with respect to the areas adjacent to the desired beam. As a result, the RX for each beam receives undesired signals from other beams simultaneously with those of its own beam.

The spectrum on the return link is shown in Fig. 4 for a three-beam system when the terminals are in access mode and located at points *a*, *b*, and *c*. The desired and undesired signals corresponding to each beam are then placed into the same frequency band on the feeder link and are sent to the common TX and HPA in the last stage of the payload.

The following analysis of this situation in which undesired signals are mixed in with desired ones clarifies the operating points of payload units and the changes in their levels in the face of traffic variation.

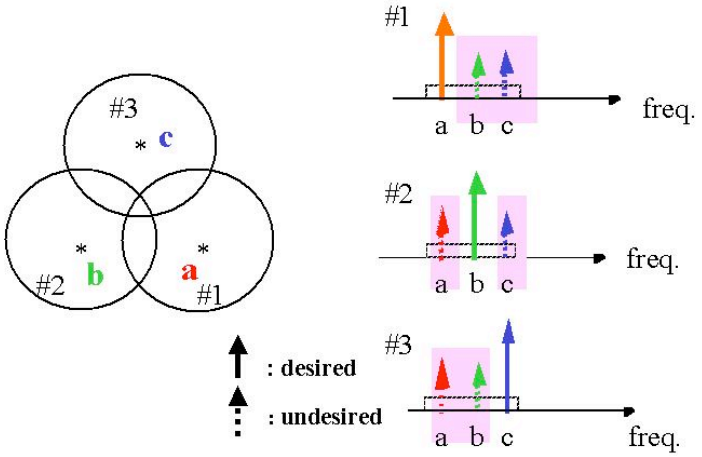

Fig. 4 Undesired signals from adjacent beams are mixed in with desired signals on the return link.

A. Multiple Circular Beams and Antenna-Pattern

An example of beam allocation in a multibeam system in which multiple circular beams cover service areas is shown in Fig. 5. Here, areas where beams overlap exist because the radiation pattern of the antennas is not steep. We investigate the case in which multiple service areas are each covered by a beam and all beams have the same circular shape. The radiation pattern represented by antenna gain *Ar(u)* for a circular aperture plane is generally given by the following equation.[3]

$$Ar(u) = \left\{ Jn(u)/u^n \right\}^2 \quad u = K \cdot a \cdot \sin(\theta), \qquad K = 2\pi / \lambda \tag{1}$$

Here, u normalizes the angle from the normal direction in terms of the antenna's aperture plane diameter and signal wavelength λ. θ is the angle from the main axis, n is a value representing the luminance distribution of the wave source, and Jn is an nth-order Bessel function with respect to this n.

Relative gain $\Delta Ar(u)$ at a point u with respect to beam center point is given by the following equation.

$$\Delta Ar(u) = Ar(u) / Ar(0) \tag{2}$$

The beam relative gain pattern and beam allocation can therefore be expressed using both u_e, the distance to beam edge, and u_S, the distance between the center points of adjacent beams, as parameters. Moreover, if we normalize u_s in terms of u_e and define this as $Q = u_S/u_e$, then Q is determined only by the beam-edge angle θ_e and adjacent-beam center angle θ_S as shown next.

$$Q = \sin(\theta_S) / \sin(\theta_e) \tag{3}$$

The relationship between $\Delta Ar(u)$ and u in the case of a uniform luminance distribution (n=1) of the wave source is shown in Fig. 6. The first null point is at u=3.8 and the first side lobe is in the vicinity of u=5. In a practical multibeam satellite system, $u=u_S<3$ and isolation with respect to adjacent areas is less than 15 dB.

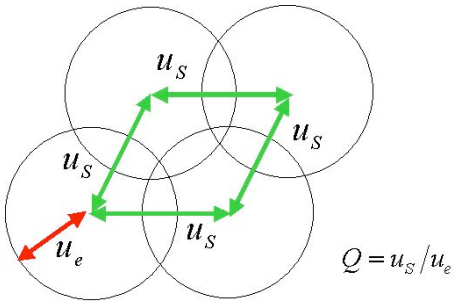

Fig. 5 Multiple circular beam configuration and definitions of its parameter.

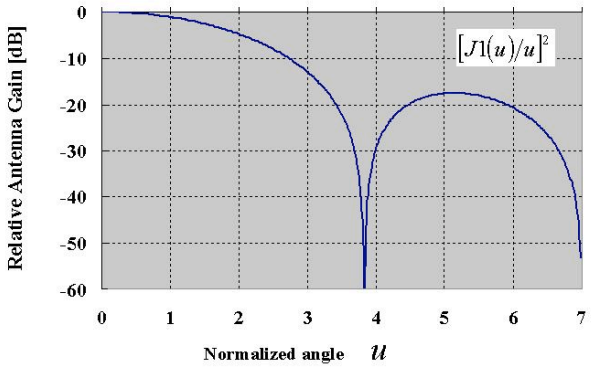

Fig. 6 Relative antenna gain $\Delta Ar(u)$ vs normalized angle u (uniform luminance n=1).

B. Transmission Characteristics of Return Link

We define the transmission characteristics for the receivers (RX), combiner (COM), and transmitter (TX) on the return link payload as $(Gr)_i$, $(Gc)_i$, (for beam #i) and Gt, respectively, the output powers of the same as $(Pr)_i$, Pc, and Pt, respectively, and the number of beams as N.

The COM has N inputs and one output. Indicating the payload input for each beam as $(Pin)_i$, the output power $(Pr)_i$ at each section of the RX can be given by the following equation.

$$(Pr)_i = (Gr)_i \cdot (Pin)_i \tag{4}$$

This leads to the following equations.

$$P_C = \sum_{i=1}^{N} (Gc)_i \cdot (Pr)_i = \sum_{i=1}^{N} (Gc)_i \cdot (Gr)_i \cdot (Pin)_i \tag{5}$$

If we assume that the RX and COM characteristics are identical for all beams and expressed as Gr_0 and Gc_0, the input power $P_{HPA,in}$ to the HPA becomes as follows.

$$P_{HPA,in} = Pt = Gt \cdot P_C = Gt \cdot Gc_0 \cdot Gr_0 \cdot \left(Pin\right)_{total} \tag{6}$$

where

$$\left(Pin\right)_{total} \equiv \sum_{i=1}^{N} \left(Pin\right)_i \tag{7}$$

Among the units inside the payload, the HPA has characteristics especially dependent on input signal level (as shown later in Fig. 11). From the above equation, the change in $P_{HPA,in}$ can be determined by finding the change in the sum total of Pin input power values from each beam.

C. Total Input Power and Traffic Distribution

Given that the satellite is currently being accessed by M terminals, let the effective isotropic radiation power (EIRP) of the kth terminal be $(EIRP)_k$; the gain with respect to terminal k of the satellite receiving antenna for beam #i be $Ar_{i,k}$; the propagation loss and distance between the satellite and each terminal be $L_{i,k}$ and $r_{i,k}$, respectively; and the wavelength be λ_i.

The input power of beam #i of the satellite is therefore given by the following equation[4] as shown in Fig. 7.

$$(Pin)_i = \sum_{k=1}^{M} \frac{(EIRP)_k}{L_{i,k}} \cdot Ar_{i,k}, \; L_{i,k} = \left(\frac{4\pi \cdot r_{i,k}}{\lambda_i}\right)^2 \tag{8}$$

Assuming now that the terminals currently accessing the satellite have a distribution density of $\rho(s)$ within a small service area dS, Eq. (8) can be expressed in an integral form over the total service area.

$$(Pin)_i = \oint_S \left\{ \frac{\rho \cdot (EIRP)_s Ar_{i,s}}{L_{i,s}} \right\} dS \tag{9}$$

On the other hand, the total number of access channels M can also be obtained by integrating $\rho(s)$ over the total service area as follows.

$$M = \oint \rho \cdot dS \tag{10}$$

The value of Eq. (9) changes for different distributions of access terminals in the service area. Assuming that each terminal has the same EIRP expressed as $EIRP_0$, and that the deviation in distance $r_{i,s}$ and λ_i between each terminal and the satellite is very small, resulting in uniform propagation loss L_0, the change in the traffic distribution can be modeled in terms of the change in antenna gain $Ar_{i,s}$ and the change in terminal distribution density ρ.

Total payload input power $(Pin)_{total}$ from all beams can be determined by Eq. (11) as a summation of $(Pin)_i$ from $i=1$ to N, where N is the total number of beams and $\alpha = EIRP_0/L_0$.

$$(Pin)_{total} = \sum_{i=1}^{N} (Pin)_i = \alpha \cdot \sum_{i=1}^{N} \left\{ \oint \rho \cdot Ar_{i,s} \cdot dS \right\} \tag{11}$$

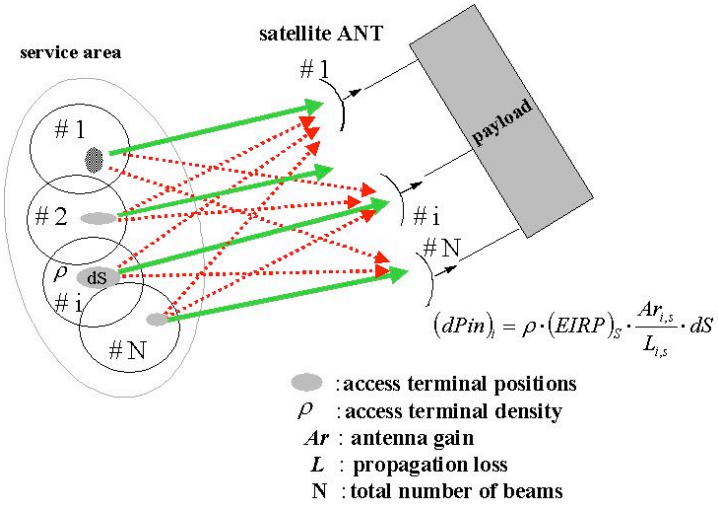

Fig. 7 Payload input power and traffic distribution.

IV. Effect of Beam Couplings on Return Link Characteristics

Using the analytical models presented in the previous sections, the change in total input power $(Pin)_{total}$ with respect to various distributions of access terminals for any case of multibeam configuration can be obtained. It is therefore possible to analyze the change in the characteristics of the payload due to adjacent-beam couplings when the traffic distribution changes.

In an actual case, the effect of next adjacent beams (beams adjacent to adjacent beams) or even farther beams are very small,[5] then it is enough to consider only the effects of adjacent beams.

A. Input Power Changes for Typical Examples with Different Traffic Distributions

Different traffic distributions in the multibeam (7 beams) configuration studied here are shown in Fig. 8. Type-I represents the special case in which each beam is ideally isolated and all access terminals are equally concentrated at beam centers where the antenna gain is maximum. The total input power of this type is used as the reference value for comparison with the other type later.

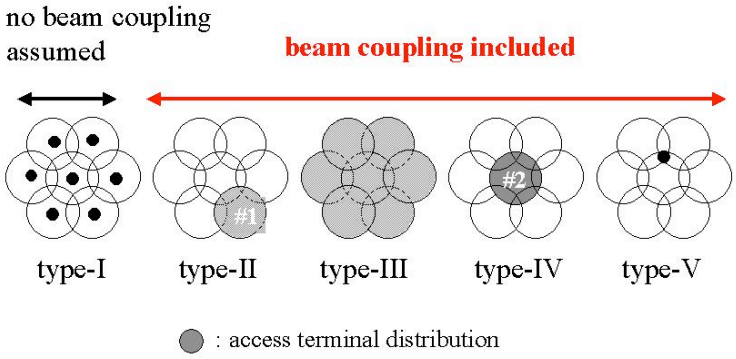

Fig. 8 Traffic distribution patterns for seven-beam system.

Type-II represents traffic uniformly distributed within a specific beam (#1); Type-III represents traffic uniformly distributed throughout all areas; Type-IV represents all traffic concentrated at the center beam #2; and Type-V represents traffic concentrated at a point within an area where three beams overlap.

The total input power with respect to various traffic distributions can be obtained by integrating over the total service area using Eq. (11). The beam antenna gain and beam allocation can be expressed using both u_e, the distance to beam edge, and u_s, the distance between the center points of adjacent beams.

The input power vs beam edge angle u_e with $Q(=u_s/u_e) = 1.6$ for different traffic distributions is shown in Fig. 9. The input power is normalized in terms of the input power for Type-I. The input power changes dependent on traffic distribution and becomes larger than that for Type-I. The input power vs beam separation Q with u_e=1.6 for different traffic distributions is shown in Fig. 10. The maximum theoretical value of Q is $\sqrt{3}$ to closely cover service area leaving no space among beams. Therefore, Q=1.6 is a practical value allowing for a margin of error. The results indicate that in the cases of traffic concentrated in one beam, input power is greater when traffic is concentrated in the beam (#2) positioned in the center rather than a beam (#1) on the periphery. The range of input power change for traffic distributions reaches a maximum of 4.5 dB in case of u_e=1.3 and Q=1.6, and 2.7 dB in case of and u_e=1.6 and Q=1.6. From the above, we can see that in a multibeam payload, multiple beams that cover service areas are in close proximity to each other and sufficient inter-beam isolation cannot be obtained. As a result, signals from terminals that exist in adjacent beams become mixed. Therefore, the total power input to the payload is greater than that for Type-I in which sufficient inter-beam isolation is assumed. In addition, it becomes relatively large when traffic is concentrated in an area where multiple beams overlap (Type V) or concentrated in a specific beam surrounded by many beams (Type IV). When traffic is concentrated in one beam for a peripheral service area (Type-II) or uniformly distributed across all service areas (Type III), the total power input to the payload is not too large, but still larger than that for Type-I.

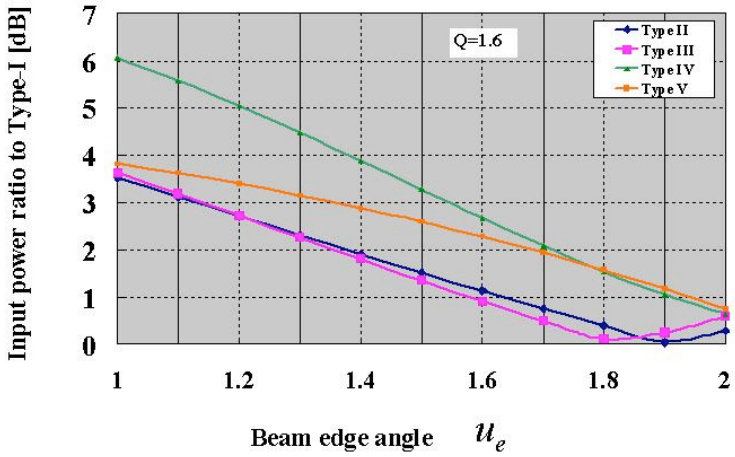

Fig. 9 Input power vs beam edge angle u_e for different traffic distributions.

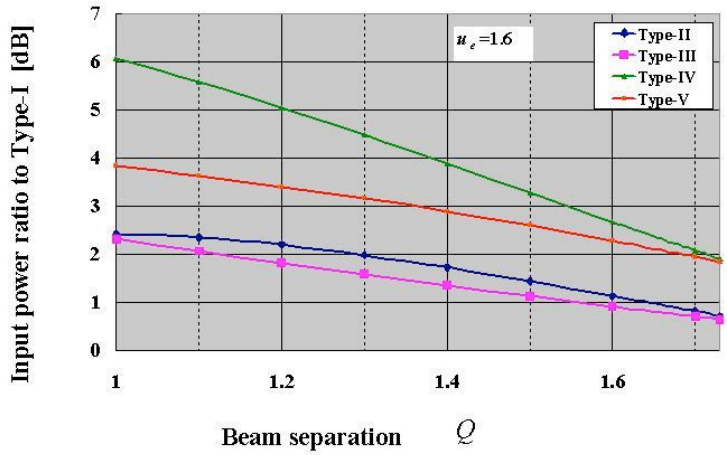

Fig. 10 Input power vs beam separation $Q(=u_s/u_e)$ for different traffic distributions.

B. Linearity Degradation

The HPA input power $P_{HPA,in}$ in the last stage of the return link payload shown in Fig. 3 can be estimated from Eqs. (6) and (11). The HPA is normally set near the limit of allowed linearity characteristics due to restrictions in power consumption. Accordingly, it has the most critical linearity characteristics among the units in the payload.

As a typical example of an HPA, Fig. 11 shows output power *Pout*, Noise-power ratio *NPR*[6], and power-consumption *Pdc* vs input power $P_{HPA,in}$, which were obtained from our measurement of an S-band 20-W solid state power amplifier (SSPA). *NPR*, which is a measure of linearity, falls at a rate of twice the increase in input power (dB) in the linear region. It can also be seen that power consumption increases with input power.

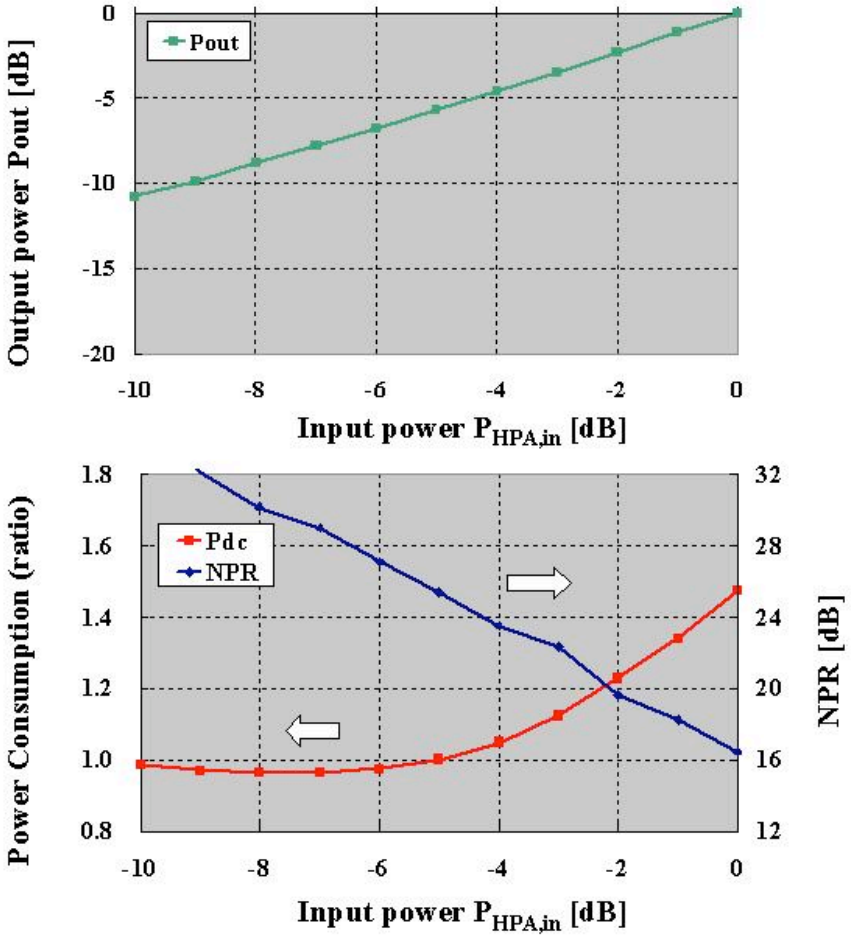

Fig. 11 Example of solid state high power amplifier characteristics (our measured data of S-band 20W SSPA).

As a design example, if we set the operating point as $P_{HPA,in}$ = - 4.7 dBm so that the target characteristics (*NPR*>25 dB) are satisfied for Type-I, NPR in SSPA falls from 25 dB when the input level changes as a result of a change in the traffic distribution. Specifically, from the characteristics shown in Fig. 11, *NPR* for Type-IV becomes 16.4 dB and 19.2 dB for u_e=1.3 and 1.6, respectively. Table 1 summarizes how the characteristics change with different traffic distributions. As shown, *NPR* degradation is around 8 dB at maximum, which can lead to degraded communications quality.

Therefore, to satisfy the target characteristics (*NPR*>25 dB) for the worst case scenario (Type-IV), a more powerful HPA is necessary for an increase in input power of 4.5 dB or 2.7 dB, which means an increase in power consumption of about 2.8 or 1.9 times.

Table 1 Typical change of payload characteristics for different traffic distributions

Beam configuration	Traffic pattern / Items	Type-I	Type-II	Type-III	Type-IV	Type-V
$u_e = 1.3$ $Q = 1.6$ $\Delta Ar = -2\,dB$	$\Delta Pin(dB)$	0	2.3	2.3	4.5	3.2
	$NPR(dB)$	24.4	20.0	20.0	16.4	18.6
	$\Delta NPR(dB)$	0	-4.4	-4.4	-8.0	-5.8
	$Pdc(ratio)$	1	1.2	1.2	1.45	1.3
$u_e = 1.6$ $Q = 1.6$ $\Delta Ar = -3\,dB$	$\Delta Pin(dB)$	0	1.1	0.9	2.7	2.3
	$NPR(dB)$	24.4	22.7	23.0	19.2	20.0
	$\Delta NPR(dB)$	0	-1.7	-1.4	-5.2	-4.4
	$Pdc(ratio)$	1	1.06	1.05	1.22	1.2

V. □ Effective Beam Allocation and Payload Design for Increasing the Number of Access Channels

In actual operation, it is difficult to determine the locations of access channels within multiple beams and then to identify the traffic distribution pattern as shown in Fig. 8. As seen from the previous study, a more powerful HPA must be installed or the maximum number of access channels must be decreased in order to guarantee communications performance and to maintain both required *NPR* and output power even for the worst case distribution. Neither of these alternatives is desirable in terms of economical system construction.

The following discusses methods for configuring and designing a beam allocation and a payload system that can suppress the range of input power change, respond flexibly to changes in traffic, and maximize the number of access channels.

A. Beam Allocation Design

Increase in input power becomes large when traffic concentrates in an area enclosed by many adjacent beams or in an area where multiple beams overlap. Accordingly, assigning the peripheral beams within a group of beams to the regions of normally heavy traffic is advantageous for increasing the number of return link access channels.

For example, if we arrange the beam pattern with u_e=1.3 and Q=1.6 like in Type-IV, in which traffic concentrates in the center beam as shown in Fig. 12(a), the variation in total input power is 4.5 dB. However, if we design the pattern like Type-II as shown in Fig. 12(b), the variation is reduced to 2.3 dB, and as a result, the number of return link access channels can be increased by a factor of 1.66 (2.2 dB).

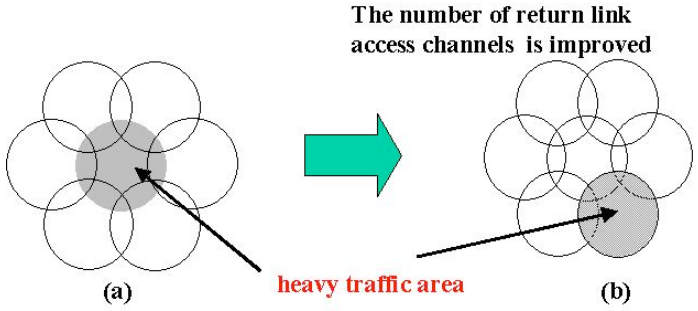

Fig. 12 Effective beam allocation.

B. HPA Operating-Point Control

From the study results, it is found that the number of access channels needs to be decreased when traffic concentrates at a particular location, and more access channels can be accommodated in the case when traffic concentrates in a beam for a peripheral service area or becomes uniformly distributed across all services areas.

Moreover, although it is possible to keep the HPA input level constant with the AGC function, it is not possible to achieve the required output power since the overall gain of the payload is changing.

The practical control method is to limit a new access when HPA input power reaches a value that corresponds to the tolerable linearity limit by monitoring HPA input power. Thus, by controlling the number of access channels so as to operate the HPA at its allowed limits, the required characteristics can always be satisfied and the maximum number of access channels can be obtained for each traffic pattern.

The maximum number of access channels vs traffic distribution when using the above method is shown in Fig. 13. These results are presented with Type-IV as a reference, and compared with the method that unconditionally limits the maximum number of access channels, which is determined for the worst case (Type-IV) and performs with no HPA monitoring. The proposed method makes it possible to increase the maximum number of access channels for traffic-distribution types II, III and V.

Since it is relatively easy to monitor the value of HPA input power, the proposed control method can be achieved by terrestrial monitoring via telemetry signals. Consequently, this method is considered practical and effective for increasing the maximum number of access channels, when traffic or link conditions are slowly time-varying. However, when traffic or link conditions are quickly fluctuating, on-board processing will be necessary to shorten the control delay.

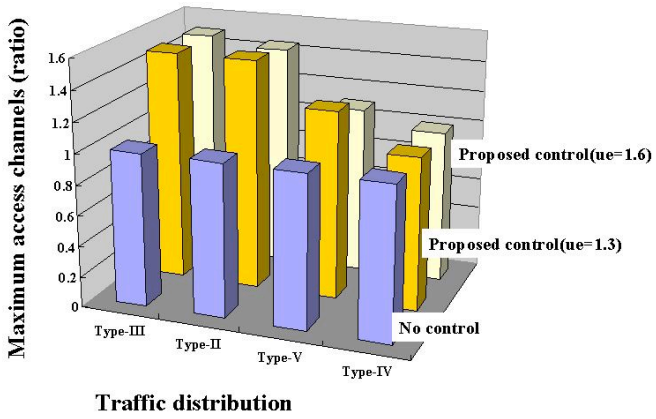

Fig. 13 Increase in maximum access channels by controlling HPA operating point.

VI. Conclusion

This paper has presented a theoretical analysis of the transmission characteristics in the return link of an interactive multimedia multibeam satellite communications system, taking beam couplings into account, and using this method, has investigated the effects of leakage from adjacent beams and the relationship between traffic distribution and change in transmission linearity.

It was found for the return link that undesired signals from adjacent beams become mixed with desired signals and the total power input to the payload changes according to the traffic distribution, since sufficient antenna isolation cannot be achieved among beams in an actual system. Moreover, on the basis of a specific system example, this change was found to cause a degradation in communications quality and a decrease in the maximum number of access channels. Accordingly, effective methods were discussed for allocating beams, designing a payload system, and controlling and operating the system so as to increase the maximum number of access channels in a multibeam payload. The study will be useful for constructing an interactive multimedia multibeam satellite communications system in an economical manner.

References

[1]Digital Video Broadcasting (DVB), "Interaction Channel for Satellite Distribution Systems," ETSI EN 301 790, European Telecommunications Standards Institute, Vol. 1.2.2, 2003, pp. 200-12.

[2]Grami, A., Gordon, K., and Shoamanesh, A., "ANIK F2 Ka-Band System: High–Speed Internet Access," *AIAA 20th ICSSC*, AIAA Paper 2000-1258, 2000, pp. 64-71.

[3]Johnson, Richard C., *Antenna Engineering Handbook*, 3rd ed., McGraw-Hill, 1961, pp. 2-20.

[4]Miya, K., *Satellite Communications Technology*, The Institute of Electronics, Information, and Communication Engineers (IEICE), 1980.

[5]Tanaka, M., and Yamamoto, H., "Linearity Degradation Due to Beam Coupling in a Multibeam Mobile Satellite Communications System," *Electronics and Communications in Japan*, Part 1, Vol. 82, No. 5, 1999, pp. 1-15.
[6]Pritchard, W. L., and Sciulli, J. A., *Satellite Communication Systems Engineering*, Prentice-Hall, Inc., 1986.